DOE/ET/53088-23

IFSR #23

FORWARD RAMAN INSTABILITY AND ELECTRON ACCELERATION

T. Tajima, C. Joshi*, J.M. Dawson*,
H.A.Baldis†, and N.A. Ebrahim‡

May 1981

*Center for Plasma Physics and Fusion Engineering
University of California
Los Angeles, California 90024

†Division of Physics
National Research Council of Canada
Ottawa, Canada K1A0R6

‡Department of Engineering and Applied Science
Yale University
New Haven, Connecticut 06520

Forward Raman Instability and Electron Acceleration

T. Tajima
Institute for Fusion Studies
University of Texas
Austin, Texas 78712

and

C. Joshi and J. M. Dawson
Center for Plasma Physics and Fusion Engineering
University of California
Los Angeles, California 90024

and

H. A. Baldis
Division of Physics
National Research Council of Canada
Ottawa, Canada K1AOR6

and

N. A. Ebrahim
Department of Engineering and Applied Science
Yale University
New Haven, Conn. 06520

It is demonstrated by particle simulations and experiments that the forward Raman instability is capable of producing extremely high energy electrons in an underdense plasma. The instability has a high saturation level for the electrostatic wave component. Its consequences/applications to the laser electron accelerator and the laser-fusion pellet preheat are discussed. The concept of the two-beam beat laser accelerator is presented.

PACS numbers: 42.65. Cq, 52.35. Mw, 52.25. Ps, 52.60. + h.

Although Raman backscatter has been under active investigation lately[1], the Raman forward scattering (RFS) instability has hitherto received relatively little attention[2]. We demonstrate, however, in this Letter that RFS can dominate backscatter when the pump is reasonably strong and/or the electron temperature is high for underdense plasmas. Furthermore, the forward scattering process results in extremely relativistic electron generation. Thus the Raman forward scattering instability warrants a serious investigation since it plays an important role in the laser electron accelerator concept[3] as well as being a significant source of laser-fusion pellet preheat. In this Letter we present results of relativistic electromagnetic particle simulations of the RFS process and results from an experiment which looks directly at forward emitted electrons from a plasma produced by an intense laser beam incident on a thin carbon foil; the calculations and experimental results are in good agreement.

In a previous paper on laser electron accelerator[3], the very short duration laser pulse acts as a photon bullet in the plasma exciting a wake of intense plasma oscillations whose phase velocity equals the group velocity of the light pulse. In such a case the Raman backscattering instability can be ignored since the backscattered wave propagates out of the incident laser packet before it experiences significant gain. The original laser electron accelerator calls for a very short pulse ($L_t \simeq \pi c/\omega_p$), not easily achieved with today's technology. Because of this we now consider the concept of laser beat accelerator, where two parallel laser beams ω_o, k_o and ω_1, k_1 are injected into an underdense plasma with the condition $\omega_p = \omega_o - \omega_1$, where ω_p is the electron plasma wave (epw) frequency. If the lower frequency beam ω_1 is noise, the process is an instability (the forward Raman instability). Cascade resonant excitation of the plasma waves has been discussed by Cohen et al[4] and

Rosenbluth and Liu[5].

Simulations were carried out on the relativistic electromagnetic particle code[6] with the periodic boundary conditions where similar wave set-ups were used as before[3] with an initially thermal and uniform plasma. Figure 1(a) shows the phase space of electrons accelerated by the beat plasma wave $\omega_p = \omega_o - \omega_1$ and $k_p \simeq \omega_p/c = k_o - k_1$, where two parallel laser beams ω_o, k_o and ω_1, k_1 are injected from the bottom. Instead of having a stretched phase space tongue (high energy electrons) just behind the short pulse laser packet[3], we now have a high energy tongue in every ridge of each wavelength of the resonantly excited plasma wave. In this particular case the parameters are: $\omega_o = 4.29\ \omega_p$, $\omega_1 = 3.29\ \omega_p$, the electron thermal velocity $v_e = 1\ \omega_p\Delta$, the speed of light $c = 10\ \omega_p\Delta$, the system length 1024Δ and 10240 particles and each beam amplitude v_i is given by $eE_i/m\omega_i = c$ ($i = 0$ or 1) with Δ being the grid spacing. The maximum electron energy reached was 85 mc^2, which is a little higher than the theoretical value of

$$W^{max} = 2mc^2[1 - (\omega_0 - \omega_1)^2/c^2(k_0 - k_1)^2]^{-1} \sim 2mc^2(\omega_o/\omega_p)^2 \qquad (1)$$

One reason for this discrepancy may be that we have now two intense electromagnetic waves so that magnetic acceleration associated with $v_o \times B_1$ and $v_1 \times B_o$ also begins to play a role[7]. The distribution function $f(p_\parallel)$ or approximately $f(\gamma_\parallel)$ is shown in Fig. 1(b), exhibiting intense main body heating as well as an extremely energetic tail. Figures 2(a) and (b) show the electromagnetic energy spectra of the system at two different times. At the earlier time the originally two-peaked structure (at k_o and k_1) already shows a downward cascade, while some small amount of energy is up-converted. The spectrum is sharply peaked at particular discrete wavenumbers $k_n = k_o - nk_p$ where n is an integer. The spectral density $S(k,\omega)$ (not

displayed here) for the electrostatic component shows no significant energy in any frequency at the backscatter $k_b = 1.77\ k_o$ or $1.3\ k_o$. This strongly suggests that all possible backscattering processes are suppressed or saturated at a very low level in our present problem. The electrostatic spectral density $S(k,\omega)$ at the resonant plasma wavenumber $k = k_p$ is very intense with some energy at the multiple harmonics $k = nk_p$. All these observations confirm that the downward photon cascade is due to the multiple forward Raman scattering.

We believe the reason why backscattering is suppressed is the following. When the backscattering electrostatic plasma wave is excited, heavy Landau damping or electron-trapping by this plasma wave saturates this wave at a low level thus limiting the backscattering to a small value. The phase velocity of the plasma wave is $v_p = \omega_p/k_b$, which for this case is $\sim 1.31\ v_e$. Thus this wave is heavily Landau damped to begin with and as it grows in amplitude, more and more particles will be trapped by it and the damping will grow. The trapping width is given approximately[8] by $\Delta v_t = (2eE_{epw}\ v_p/m\omega_p)^{\frac{1}{2}}$, where E_{epw} is the electric field for the plasma wave. The condition that a large number of electrons are trapped is given[9] by $v_p - \Delta v_t \lesssim 2v_e \equiv 2(T_e/m)^{\frac{1}{2}}$. The maximum electrostatic wave intensity is obtained for a cold plasma by setting $v_e = 0$. This gives for the saturation amplitude E_{epw} for the longitudinal wave as

$$\frac{eE_{epw}}{m\omega_p} = \frac{c}{4}\ \frac{\omega_p}{\omega_o} \qquad (2)$$

For our case, the phase velocity is $O(v_e)$ and we expect little growth; in any case, the intensity given by (2) is only 0.02% of the light waves. In addition the two plasmon decay instability would also saturate at a low level even if ω_o were chosen to be $2\omega_p$ because strong Landau damping sets in much earlier for $2\omega_p$ decay than it does for the forward Raman process. The forward

Raman process is the last process to saturate in this underdense plasma. In fact it can be argued that it will saturate only when the original electromagnetic wave has completely cascaded to waves near $\omega = \omega_p$; in the process the bulk of the plasma is heated to a temperature of mc^2. The maximum energy conversion efficiency from the electromagnetic waves to electrostatic waves and ultimately to heat may be estimated as $\eta_{max} = 1 - (\omega_p/\omega_o)^2$. If two dimensional effects are taken into consideration, side scattering can play an important role. One must also include effects of self-focussing so that a detailed analysis of real situations will be quite involved.

As we shall see below, Raman forward scattering can take place even with a single beam, (the Raman forward scattering instability); however, it needs a longer time/system and/or higher density to be significant for growth from noise. Also, in the one beam case forward scattering at non-zero angles may be important and more complete multidimensional treatment is called for. It is this effect that may pose a serious problem to the beam propagation in large low density plasmas in a target chamber for laser fusion[10].

The role of Raman forward scattering in relativistic energy electron generation is investigated experimentally and checked against particle simulation using the same relevant parameters. 130 Å thick, self-supported carbon foils were irradiated at normal incidence by intense, $v_o/c \sim 0.3$, 700 pS FWHM, CO_2 - laser pulses. 50% of the incident energy was typically transmitted by the plasma. Thus it can be assumed that the foil plasma becomes underdense around the peak of the laser pulse. The electron temperature of the bulk distribution was deduced from the slope of the ion spectra recorded absolutely using Thomson parabolas, to be ~ 20 keV for both front and the rear expansion. In Figure 3, we show the absolute electron spectra measured at $\theta \simeq 5°$ in the forward

direction. If a Maxwellian distribution is assumed, then these distributions can be characterized by temperatures of 90-100 keV. Electrons with energies up to 1.4 MeV were observed in the forward direction. For comparison, in the backward direction the electron spectra had characteristic temperatures of 50 keV with maximum energies of 600-800 keV. In the forward direction the highest energy (> 1 MeV) electron emission is strongly peaked in the direction of the laser. Electrons up to 400 keV are observed nearly isotropically, probably attributable to $2\omega_p$ decay and Raman sidescattering. A simple estimate shows that RFS is important in our experiment. The growth rate for the four-wave process (i.e., direct forward scatter) is given by $\gamma = \frac{1}{2} (v_o/c)\ \omega_p^2/\omega_o$ and the finite length limit on growth is $\gamma L/(c\ v_g)^{\frac{1}{2}} >> 1$, where $v_g = 3\ k_p\ v_e^2/\omega_p$ and L is the interaction region length. For the above conditions with $\omega_p/\omega_o \sim 0.46$, $\gamma/\omega_o = 0.03$ and we have ~ 27 e-foldings growth from the initial noise level. For backscatter the growth rates are comparable to those for forward scatter but backscatter suffers much more severe Landau damping. The assumption of a homogeneous plasma with $L/\lambda \simeq 50$ is reasonable, since we expect the instability to occur in the density plateau region, separating the front and the rear expansions. This region has a density scale-length somewhere in between the focal spot diameter (150 μm) and the ion acoustic speed times the FWHM pulse length (1000 μm).

Simulations were carried out which match the experimental conditions by choosing $n_e/n_c = 0.216$ (i.e. $\omega_o = 2.16\ \omega_p$), $T_e = 20$ keV, $ct_e/\lambda = 61$, and $v_o/c = 0.3$ where t_e is the duration of the simulation run, λ the wavelength of the laser light, and n_c the critical density. The distribution function $f(p_\parallel)$ as well as the wave spectra are displayed in Fig. 4. The shape of the simulation distribution with $\varepsilon_{max} \simeq 1.3$ MeV is similar to the experimental one with $\varepsilon_{max} \simeq 1.3$ MeV. The backward maximum energy for simulation 0.9 MeV is compared with that for experiment ~ 0.8 MeV. The electrostatic wave

spectra [Fig. 4(b)] show that the backscattered mode (k_b) which grows initially is quickly swamped by other modes with a smaller wavenumber, the most intense of which is the forward scatter (k_p). In addition, there are some wavenumbers which are less than k_p [11]. Thus the heated electron distributions obtained by the experiment and simulation agree well and most of the electron heating is due to the forward Raman scattering process (and its subsequent process), but not so much due to the backward process.

The work was supported by DOE contracts DE-FG05-80 ET 53088 at UT, NSF grants PHY-79-01319, 4-442520-21844, and Los Alamos contract 4-XPO-1033P-1 at UCLA. Stimulating discussions with Prof. F. F. Chen, C. E. Clayton, Dr. K. Estabrook and Dr. J. M. Kindel are acknowledged with pleasure.

REFERENCES

1. D. Phillion and D. L. Banner ; Lawrence Livermore Laboratory Report UCRL - 84854 L (1980) - N. A. Ebrahim, C. Joshi and H. A. Baldis, UCLA PPG 525 to be published - R. G. Watt, R. D. Brooks and Z. A. Pietrzyk, Phys. Rev. Lett. 41, 170 (1970).

2. K. Estabrook, W. L. Kruer, and B. F. Lasinski, Phys. Rev. Lett. 45, 1399 (1980).

3. T. Tajima and J. M. Dawson, Phys. Rev. Lett. 43, 267 (1979).

4. B. I. Cohen, A. N. Kaufman, and K. M. Watson, Phys. Rev. Lett. 29, 581 (1972).

5. M. N. Rosenbluth and C. S. Liu, Phys. Rev. Lett. 29, 701 (1972).

6. A. T. Lin, J. M. Dawson, and H. Okuda, Phys. Fluids 17, 1995 (1974).

7. M. Ashour-Abdalla, J. N. Leboeuf, T. Tajima, J. M. Dawson, and C. F. Kennel, to be published in Phys. Rev. A (April, 1981).

8. The formula is nonrelativistic, but is sufficiently accurate to the present purpose. Also see the footnote in Ref. 3.

9. J. M. Dawson and R. Shanny, Phys. Fluids 11, 1506 (1968).

10. C. Joshi, C. E. Clayton and F. F. Chen, UCLA PPG 537 – to be published.
J. J. Thomson, Phys. Fluids, 21, 2082 (1978).

11. These modes would correspond to the "beam modes" generated by the forward accelerated electrons. In the single pump case of $\omega_o = 4.3\ \omega_p$, similar dominance by the forward scattering process is observed. In this case no significant electrostatic modes with $k < k_p$, however.

FIGURE CAPTIONS

Fig. 1 Photon beat acceleration by two beams (ω_o, k_o) and (ω_1, k_1). (a) The electron phase space (x, P_x) at $t = 240\ \omega_p^{-1}$. The maximum $\gamma_{\parallel}$ for electrons is 85 in this case. (b) The logarithm of the electron distribution function at $t = 135\ \omega_p^{-1}$.

Fig. 2 The electromagnetic energy distribution as a function of mode numbers. Pumps k_o and k_1 one indicated by arrows. (a) at $t = 142.5\ \omega_p^{-1}$, and (b) at $t = 240\ \omega_p^{-1}$.

Fig. 3 Experimental electron energy distributions in the forward and backward directions. Shows three different shots.

Fig. 4 Simulation (under the same conditions as in Fig. 3) electron energies (a) at $t = 250\ \omega_p^{-1}$ as well as the electrostatic mode spectra at $t = 100\ \omega_p^{-1}$ (b).

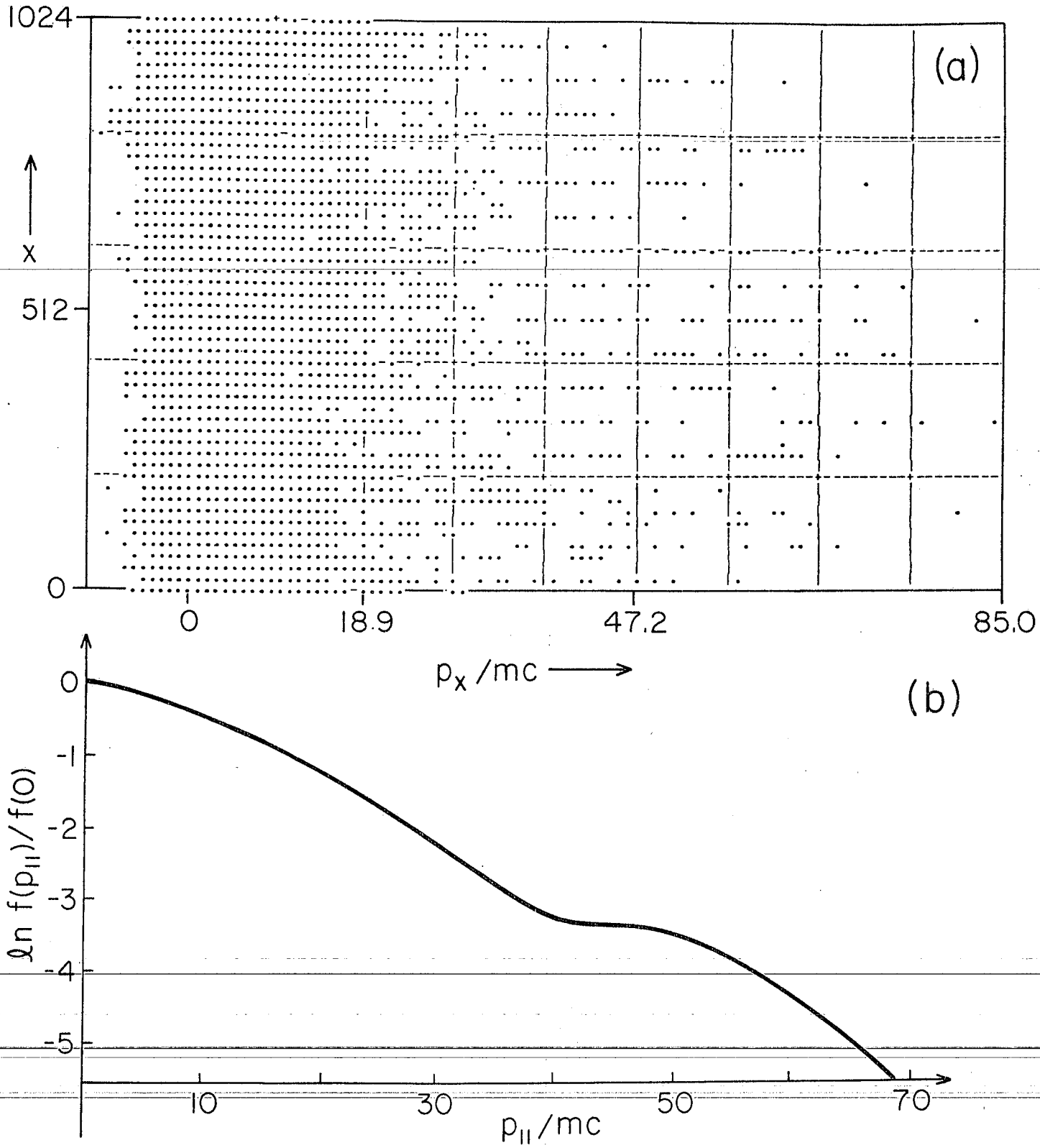
1024
512
0
X
(a)
0
18.9
47.2
85.0
p_x/mc
(b)
0
-1
-2
-3
-4
-5
$\ln f(p_{11})/f(0)$
10
30
50
70
p_{11}/mc

Fig. 1

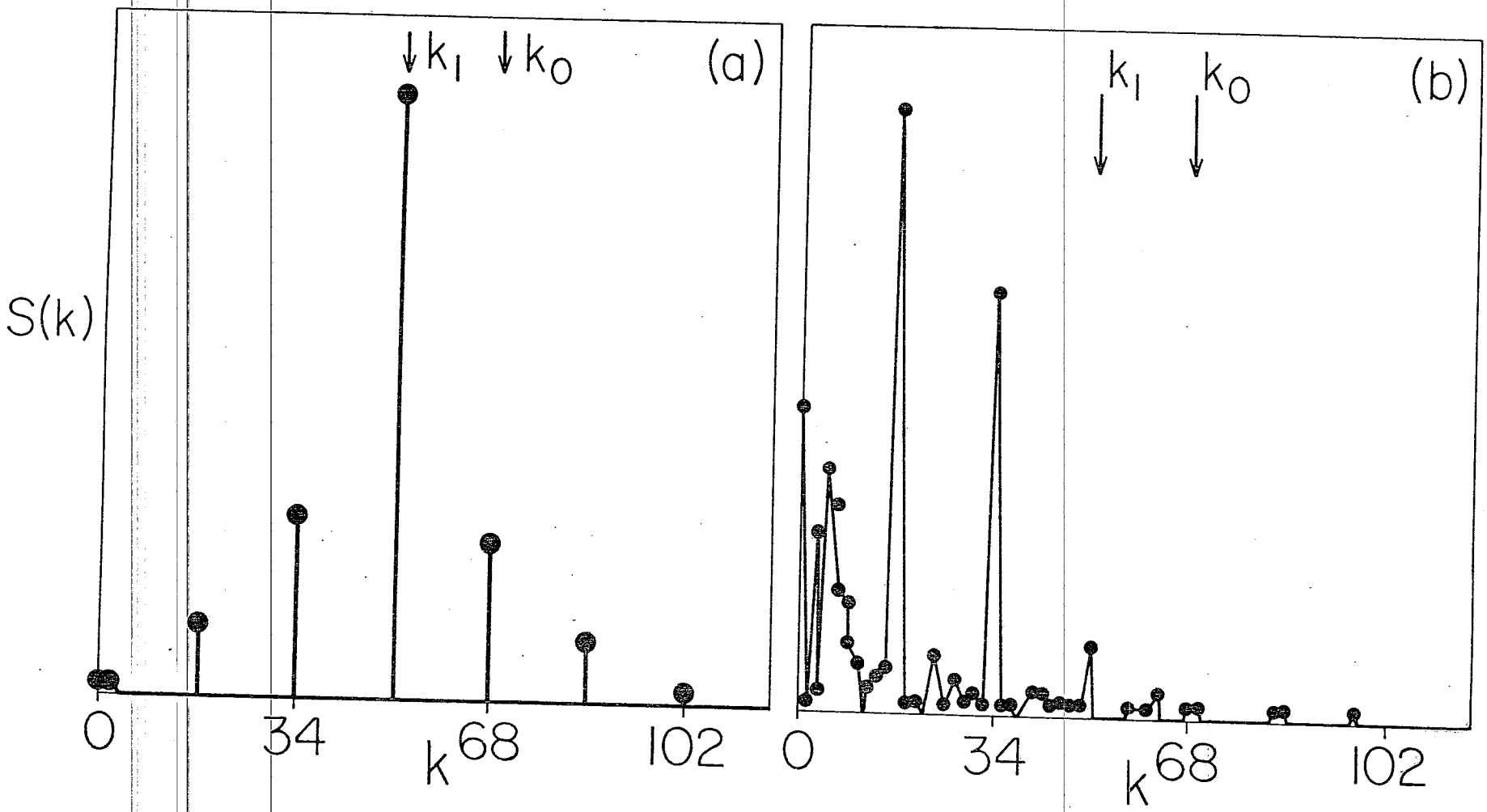

Fig. 2

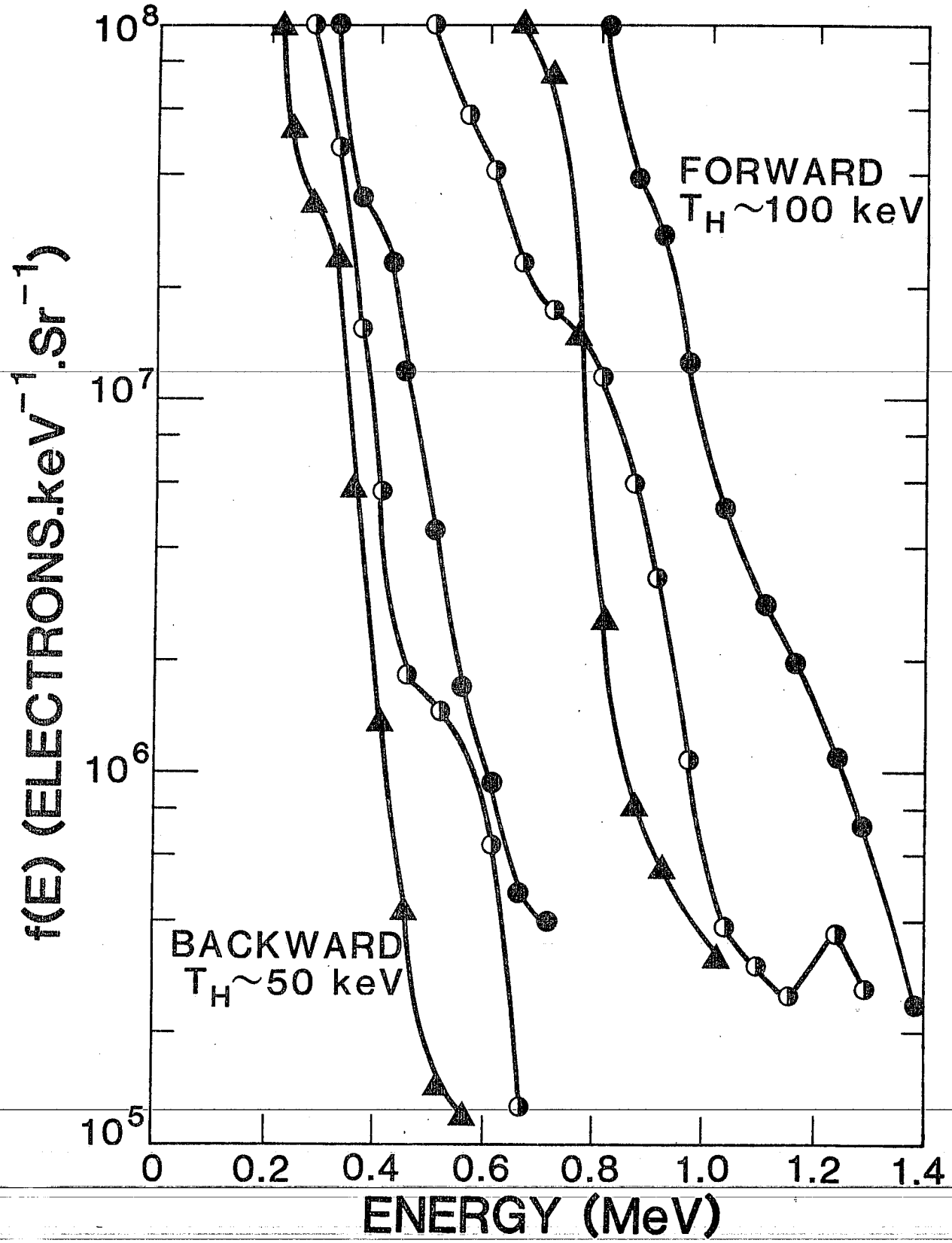
10^8
10^7
10^6
10^5
f(E) (ELECTRONS.keV^{-1}.Sr^{-1})
FORWARD
T_H~100 keV
BACKWARD
T_H~50 keV
0
0.2
0.4
0.6
0.8
1.0
1.2
1.4
ENERGY (MeV)

Fig. 3

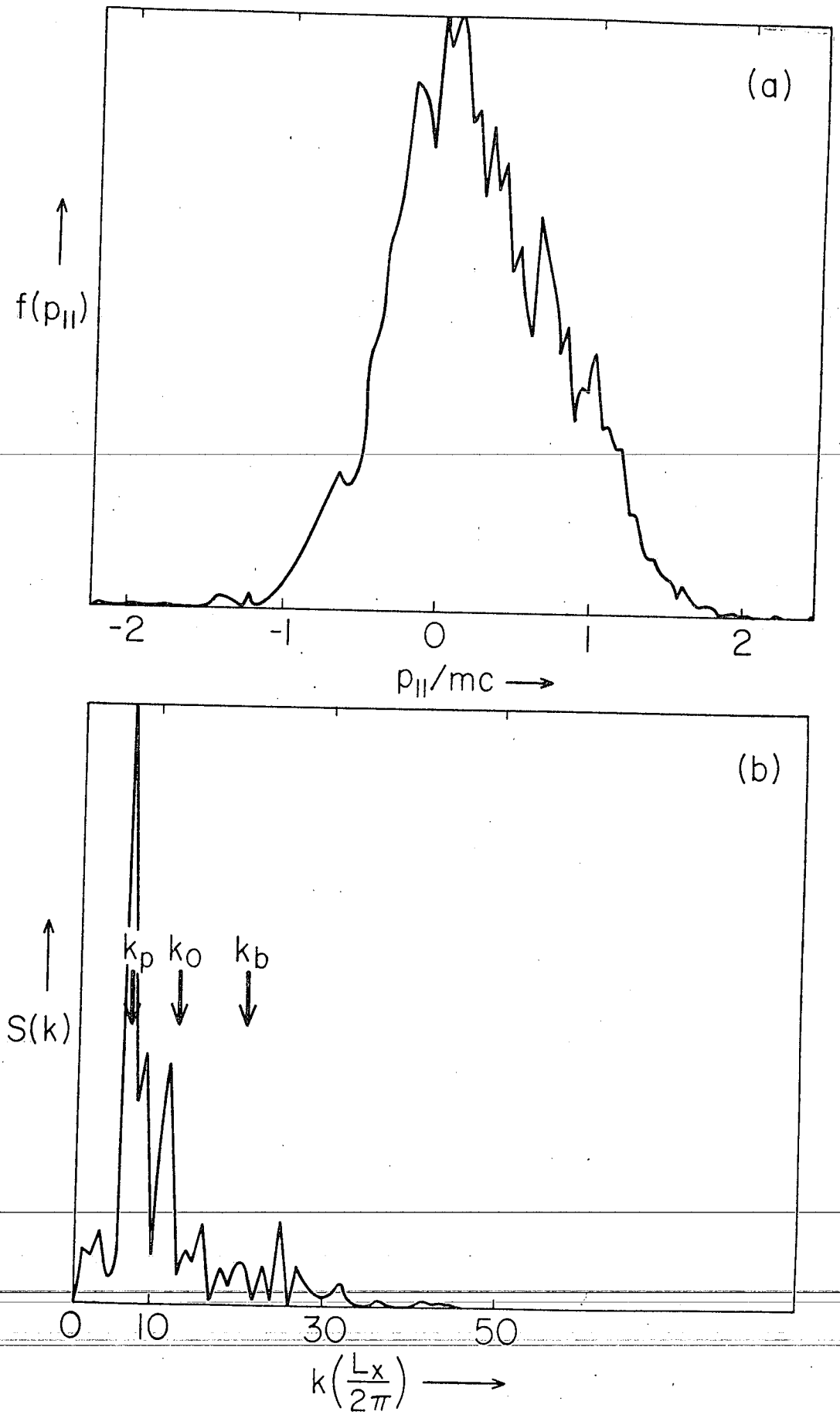
(a)
$f(p_{||})$
-2
-1
0
1
2
$p_{||}/mc \longrightarrow$
(b)
k_p k_0 k_b
$S(k)$
0
10
30
50
$k\left(\frac{L_x}{2\pi}\right) \longrightarrow$

Fig. 4